International Journal of Research in Engineering and Science (IJRES)
ISSN (Online): 2320-9364, ISSN (Print): 2320-9356
www.ijres.org Volume 10 Issue 4 ǁ 2022 ǁ PP. 01-09

Near-surface wind speed and wind turbine capacity factor in Neuquén Province, Argentina

Samuel D. Troncoso Schenker, Claudia Palese* and Jorge L. Lassig
Faculty of Engineering, National University of Comahue, Neuquén, Neuquén, Argentina

Abstract
This paper has two main objectives, to improve a part of the existing provincial wind resource potential map and to compare the gross capacity factor of different classes of commercial wind turbines. Software that implements a mass-consistent model within the atmospheric boundary layer and measurements of near-surface wind data from 18 sites was used. Also, four commercial wind turbines data were utilized. The annual wind regime and energy production of the wind turbines were obtained at a height of 120 m at each grid point (spatial resolution of 422 m). Results indicate that there are locations that have a very good to excellent wind resource to install wind farms. Zones where Class III wind turbines can be located have the largest land extension. Class II wind turbines have better performances than Class I or IIII as they have the highest annual average gross capacity.

Keywords: *Neuquén Province, wind power, wind resource map, near-surface wind speed, 50-year extreme wind speed, wind turbine capacity factor, Argentina.*

Date of Submission: 13-04-2022 Date of acceptance: 29-04-2022

I. INTRODUCTION

Wind resource maps were made in different argentine provinces because this type of cartography provides a basic tool for making wind resource development plans and facilitates the technical and economic analysis for different energy supply alternatives, becoming a support to make decisions. It allows the identification of potentially suitable areas for the development of projects and the design of studies that evaluate said resource at specific sites, both for the generation of electric power on a commercial scale in systems connected to the electric power grid and those of smaller scale in isolated systems.

These maps were made since the promotion of the renewable energy sector due to Law 27,191 "National Development Regime for the use of renewable energy sources for the production of electricity" and the bidding processes carried out through the Program for the Supply of Electric Energy from Renewable Sources (RenovAr by its acronym in Spanish) and the Regime of Term Market from Renewable Energy Sources (MAT ER by its acronym in Spanish) encouraged wind farm installation projects in the country.

Examples of provincial wind resource maps can be found in [1, 2, 3, 4]. The first three were made with measurements of anemometric towers and meteorological stations with a mass-consistent model, while [4] was produced with Merra reanalysis data. The spatial resolution of said maps exceeds a kilometre.

The knowledge of regional distribution of the gross capacity factor of wind turbines provides information from two points of view: the characteristics of the regional wind regime and the efficiency of wind turbines. In Argentina, no maps of this type have been published yet. But there is a study [5] realized in two specific sites, Bahía Blanca (Buenos Aires Province) and San Julián (Santa Cruz Province).

The studied area (Figure 1) is located in Neuquén Province, which is placed in the extreme northwest of argentine Patagonia. Since the wind resource is considerably high [6, 7, 8, 9], the provincial government encourages the installation of wind farms in order to expand the energy matrix of the area that is currently based on the exploitation of oil and gas. In addition, there are main electricity transmission lines which are a favourable condition.

The following paper has a two main objectives, one is to improve a part of the existing provincial wind resource potential map by the incorporation of new measured wind data and increasing the spatial resolution. The other goal is to build capacity factor maps to evaluate the regional distribution of the performance of different classes of commercial wind turbines.

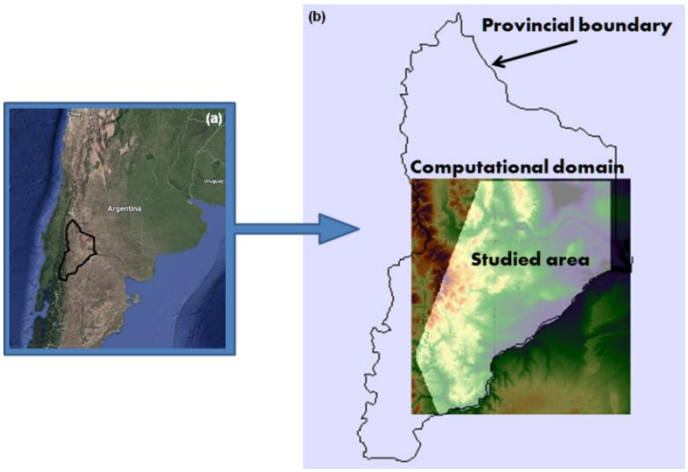

Figure1: (a) Location of Neuquén Province. (b) Computational domain that contains the studied area.

II. METHODOLOGY

The ArgentinaMap software is used to assess the wind resource. It is a mass-consistent model within the atmospheric boundary layer combined with a geographic information system. This program is a modification made by CREE (Regional Centre for Wind Energy) of the WindMap software developed by [10]. Its main characteristics can be seen in [11].

The model domain, which can be seen in Figure 1 (b), covers the area between 37° 55' S - 40° 36' S and 67° 58' W - 71° 09' W (269.5 km by 295.7 km). The upper boundary of the domain is set at an elevation of 3090 m above mean sea level (amsl), while the lower limit is defined by the surface elevations indicated by a digital elevation map. This rectangular domain contains the area of interest for the development of wind farm projects.

The data necessary to execute ArgentinaMap are: geophysical digital maps, near-surface and upper-air data of wind speed and wind direction, and the characteristics of the regional atmospheric boundary layer. Each of these aspects is summarized below.

The digital elevation model is shown in Figure 2 (a) and it was obtained from the United States Geological Service website (USGS, SRTM Data). It was converted to the projection Gauss-Krüger (Argentina, zone 2), with a horizontal resolution of $\Delta x = \Delta y = 422$ m. The lowest elevation (218 m amsl) is located in the eastern side of the map, while the highest elevation is in the western side, reaching 2806 m amsl.

The annual average aerodynamic roughness length is shown in Figure 2 (b). This map was constructed using an indirect methodology based on satellite data from the ETM+/Landsat7 sensor in which land-use/land-cover types were mapped. Then, each type was associated with a roughness length value. This map was rectified with the same spatial resolution (422 m) as the elevation map.

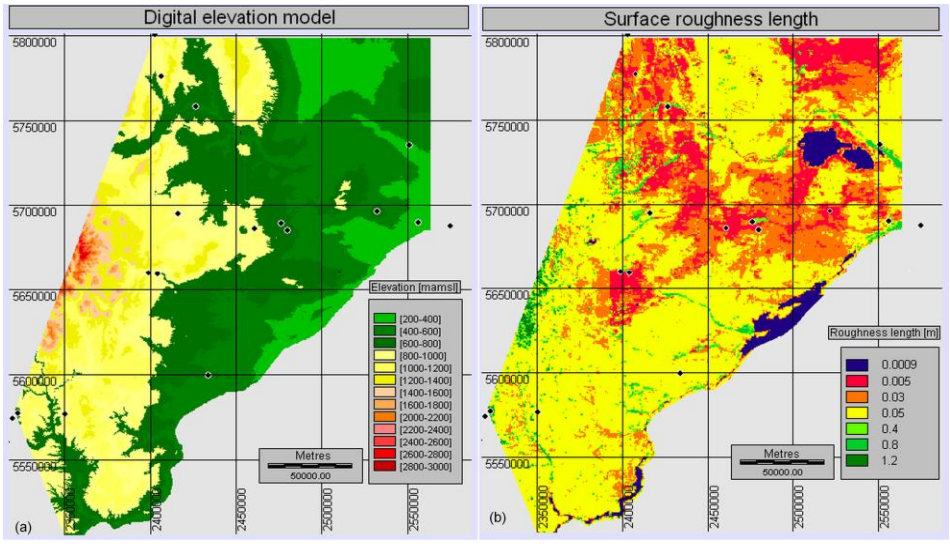

Figure 2: (a) Digital elevation model. (b) Digital map of the annual mean of the aerodynamic roughness length. The reference system used is Gauss-Krüger (Argentina). The positions of available near-surface wind speed measurement stations are also shown in both maps.

Geostrophic wind speed and wind direction at 810 m, 1510 m and 3090 m amsl come from the atmospheric model of the Global Forecast System (GFS) of the National Centre for Environmental Prediction (NCEP) of a five-year period (2000 - 2004). The analysis of these data is representative of the upper-air winds characteristics of the entire domain. They show that the most frequent winds come from the Southwest (240°) at the lowest elevation (810 m amsl), turning to the West (270°) at the highest (3090 m). The mean value of the vertical increase in wind speed in the free atmosphere is 0.004 s^{-1}. Directional analysis indicates that westerly winds are the strongest with wind speeds that vary between 7.4 and 15.2 m s^{-1} at 810 m and 3090 m amsl, respectively.

The annual mean characteristics of the local atmospheric boundary layer were calculated with the results of the same atmospheric model. The height of the transition layer is 663 m above ground level (agl) and the near-surface boundary layer height is 170 m agl. The most frequent atmospheric stability is the neutral type.

Table 1: Characteristics of the measurement stations and data used. (a) Data from this site was used as the control station.

Site	Coordinates (X; Y) [m]	Elevation [m amsl]	Sensor height [m agl]	Period [years]	Time intervals [min]	Data available [%]
Cerro Bandera (a)	2461121.260; 5686973.989	946	30	1.5	60	69
Chorriaca	2403163.315; 5801480.819	1189	10, 30	3.6	10	100
QuiliMalal	2426695.634; 5758818.025	593	10	0.67	10	98
Neuquén Aero	2574772.970; 5688520.978	272	10	31	60	71
Agua del Cajón	2555966.632; 5690852.679	307	2,5	2.2	10	98
Cutral Có	2476665.805; 5690329.742	659	10	5.3	180	45
Cerro California	2480197.668; 5685961.940	701	35	2.2	60	86
Villa PPL Escuela	2399128.735; 5660996.805	811	10	1.75	60	94
Villa PPL Cerro	2404638.970; 5660629.658	852	18	1.3	60	92
Chapelco Aero	2317422.988; 5561311.355	789	10	21	60	36
Junín Andes	2320281.826; 5575389.000	1073	26	1	10	98
Junín Andes Esc.	2323449.237; 5578114.007	784	10	9.4	1440	92
Chañar	2550898.586; 5736286.675	286	40, 60, 80	1.7	10	95
Chorriaca N	2405120.118; 5779760.000	868	40, 60, 80, 82	2	10	97
La Rinconada	2350948.249; 5577827.067	999	40, 60, 80, 82	1	10	100
Cerro Senillosa	2532203.954; 5696262.230	696	40, 60, 84	2	10	99
Subida del Capo	2416202.597; 5695908.242	1033	20, 40, 60	2	10	100
Picún Leufú	2433799.761; 5600644.489	618	40, 60, 85	2	10	97

Table 2: Summary of the wind features. (a) Annual mean wind speed corresponds to the highest level measurement. (b) Data from this site was used as the control station.

Site	Dominant direction [°]	Annual mean [m/s] (a)
Cerro Bandera (b)	270	7.4
Chorriaca	270	6.7
QuiliMalal	0	4.0
Neuquén Aero	240	3.6
Agua del Cajón	240	3.9
Cutral Có	240	6.5
Cerro California	210	6.8
Villa PPL Escuela	270	3.3
Villa PPL Cerro	270	3.6
Chapelco Aero	240	7.8
Junín Andes	270	7.7
Junín Andes Esc.	210	2.6
Chañar	270	5.9
Chorriaca N	300	5.3
La Rinconada	300	6.9
Cerro Senillosa	210	7.8
Subida del Capo	300	7.5
Picún Leufú	240	7.6

To properly represent the characteristics of wind flow through the analyzed region it is important to have high-quality near-surface level wind data from a dense network of measuring stations. This work used data from 18 sites which means that the measurement network density is high as it can be seen in Figure 2. Table 1 contains data availability and information of each site. Note that Neuquén Aero and Chapelco Aero have long-term registers, being 31 and 21 years respectively. In addition, the measurement towers of the last six sites have two anemometers installed per level and collected data from three levels or more.

A quality control of wind speed and wind direction data was applied in order to identify inconsistencies and loss of data in the records. This task included the verification of the data validity range, analysis of persistence and, when it was possible, correction of tower shadowing on anemometer data according to the methodology suggested in [12]. As there is variation in the duration of the measurement period, an analysis was carried out to verify the prediction of the climatology of the wind speed in each of the measurement stations.

A summary of the statistical analysis of the data series for each site is included in Table 2. It can be seen that the region is dominated by winds from the west sector (210° to 300°). Quili Malal has winds that often come from the North due to the channelling produced by the topography. The annual mean wind speeds at each measurement height show that Chapelco Aero (10 m agl) and Cerro Senillosa (84 m agl) have the largest wind speeds, both reaching 7.8 m s^{-1} and Junín de los Andes Escuela has the weakest wind speeds at 2.6 m s^{-1}.

The evaluation of the precision of results was done by calculating the error, εr, (equation (1)) and the correlation coefficient [13], r, between the measured and simulated wind speeds, in a directional way (12 sectors) and at the sensor height.

$$\varepsilon r = \frac{|v - v^*|}{v} \times 100 \quad (1)$$

where v = directional average measured wind speed and v* = simulated wind speed in the same direction as v and at the same measurement height of v.

Several simulations were performed with changes in configuration and initialization in order to minimize the differences between obtained values and measured data. The errors were calculated in each station at its sensor height.

In this work it was established that a simulation has optimal quality when errors were not greater than 1 % and it has poor quality when εr ≥ 10 %. The final result is reached when a simulation presents the highest occurrence of low errors and high r.

The validation of the results was done with a simulation that skips data from the control station in order to be able to compare the measured and simulated wind speed at its position. Cerro Bandera site was selected as the control station due to its central position in the domain.

The simulation was configured to obtain results at 120 m agl. Then, the resulting wind speed map was categorized according to the wind power density of Table 3.

Table 3: Categories of wind power density utilized to classify wind speed map at 120 m agl.

Category	**1**	**2**	**3**	**4**	**5**	**6**	**7**
Wind speed [m s^{-1}]	< 6.3	7.3	8.0	8.6	9.1	10.0	> 10.0
Wind power density [W m^{-2}]	< 290	450	600	740	880	1160	> 1160

2.1 CAPACITY FACTOR (CF)

The gross capacity factor (CF) of a wind turbine measures its actual production relative to its possible production and is defined as the ratio between the annual energy production of a wind turbine (E(v)) and its annual energy production while operating at its rated power for one year (E). E(v) is a product that comes from the simulation. The CF was calculated using the following equation (2) at each point of the mesh established in the domain without considering wake losses or decreases due to uncertainties.

$$CF = \frac{\sum_{v_a}^{v_c} E(v)\ W(v)}{E} \quad (2)$$

E(v) is calculated as E(v) = Pot(v) T, where Pot(v) is the power curve of the wind turbine (equation (3)) and T is set as one year. W(v) is the Weibull probability density function and it is represented in equation (4), where k and c are shape and scale parameters, respectively.

$$Pot(v) = \frac{1}{2} \rho\ v^3\ A\ Cp \quad (3)$$

where ρ = air density, v = wind speed, A = rotor area, Cp = wind turbine power coefficient delivered by the manufacturer.

$$W(v) = \frac{k}{c}\left(\frac{v}{c}\right)^{(k-1)} e^{-\left(\frac{v}{c}\right)^k} \quad (4)$$

Through the simulation, the values of E(v), v, c and k at an height of 120 m above ground level were obtained at each grid point.

Wind turbines are designed to support different wind conditions defined with base parameters such as annual mean wind speed at hub height, $\bar{v}$, 50-year extreme wind speed over 10 minutes, Vref, 50-year extreme

gust over 3 seconds, Vgust, and the mean turbulence intensity at 15 m s^{-1}, Iref. Table 4 shows the classification of wind turbines [14], with Class I being the most robust, since they support wind speeds up to 10 m s^{-1} and extreme wind speeds of 50 m s^{-1}. In this paper, the turbulence intensity used for the three classes was Category A, which is 16 %.

Table 4: Wind turbine classes

Wind turbine class	I	II	III
V average, $\bar{v}$ [m s^{-1}]	10	8.5	7.5
V reference, Vref [m s^{-1}]	50	42.5	37.5
V gust, 50-years return [m s^{-1}]	70	59.5	52.5

In this paper CF is compared in two ways. Firstly, between wind turbines that has the same rated power and different IEC Class, and then between wind turbines of the same class and different rated power. Four commercial wind turbines were chosen to compare CF at the same height and all of them have three blades upwind horizontal axis. These machines were chosen because of the availability of their power curve data, obtained from http://thewindpower.net. Rated wind speed, cut-in wind speed and cut-out wind speed are different between each type of wind turbine as shown in Table 5. Class I wind turbines have a smaller sweep area because they must withstand the stresses caused by higher wind speeds.

The power curves are shown in Figure 3. It is observed that WT III-3300 makes a better use of low wind speed while WT I-3300 does it with high wind speed.

Table 5: Characteristics of wind turbines

Wind Turbine	Rated power [kW]	Rated wind speed [m s^{-1}]	Rotor diameter [m]	Cut-in wind speed [m s^{-1}]	Cut-off wind speed [m s^{-1}]	Swept area [m^2]	Class
WT I-3300	3300	14	105	3.5	25	8659	IA
WT II-3300	3300	13	117	2.5	25	10751.3	IIA
WT III-3300	3300	12	126	2.5	22	12469	IIIA
WT III-3450	3450	11.5	126	4.5	22	12469	IIIA

Once the annual mean wind speed and Weibull parameters were obtained from the simulation at each point of the mesh, the 50-year extreme wind speed over 10 minutes or reference wind speed, Vref, was calculated at 120 m, according to equation (5).

$$\frac{Vref}{\bar{v}} = \frac{(\ln n)^{\left(\frac{1}{k}-1\right)}}{k \quad \Gamma\left(1+\frac{1}{k}\right)} \left\{ k \ln n - \ln\left[-\ln\left(1-\frac{1}{Tr}\right)\right]\right\} \qquad (5)$$

where $\bar{v}$ is the annual average wind speed at rotor height (120 m) obtained by the simulation, n is the number of independent events which is 23037, Γ () is the Gamma function and Tr is the return period, which is 50 years.

Vref was used to build a map with the (most) suitable areas to locate each type of wind turbine. In this paper, the land classification analysis excludes zones with Vref less than 30 m s^{-1} (Class IV) and areas with Vref greater than 50 m s^{-1} (Class S).

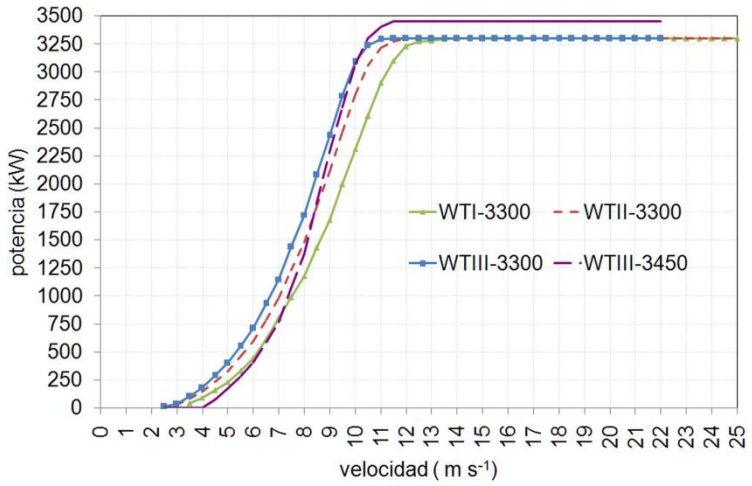

Figure 3: Power curves of wind turbines. Supplied by the manufacturer at a standard air density at sea level that is 1.225 kg m^{-3}. Source: https://www.thewindpower.net.

III. RESULTS

3.1 WIND SPEED

The annual average wind speed at 120 m agl is shown in Figure 4. It varies between 3.95 m s^{-1} and 14.66 m s^{-1}. Wind speeds that are greater than 8 m s^{-1}, are located where topography exceeds 600 m amsl. The quality achieved by comparing the measured and simulated wind speed is adequate since r = 0.94 and εr < 7 % (all wind directions). The westerly wind has εr < 4%. The error at control station is εr = 8 %.

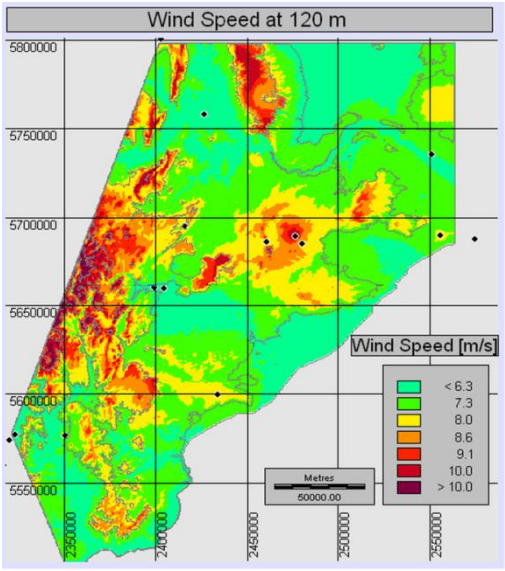

Figure 4: Annual average wind speed at 120 m agl. The limit of the analysis area and topographic levels every 500 m, starting from 500 m amsl, are also drawn on the map.

3.2 LAND CLASSIFICATION ACCORDING TO CLASSES OF WIND TURBINES

Zones that are suitable for each wind turbine class are shown in Figure 5 and these classes were defined according to Vref (Table 4). This study does not include the analysis of zones classified as Class IV (Vref < 30 m s^{-1}) and Class S (Vref > 50 m s^{-1}) in Figure 5. The predominance of the area to install Class III wind turbines can be seen on the map, and its total extension is 17,716 km^2. Class II has a total area of 10,435 km^2 and Class I has 6,579 km^2. Class S corresponds to an area where Vref exceeds 50 m s^{-1}, therefore, wind turbine needs a specific design.

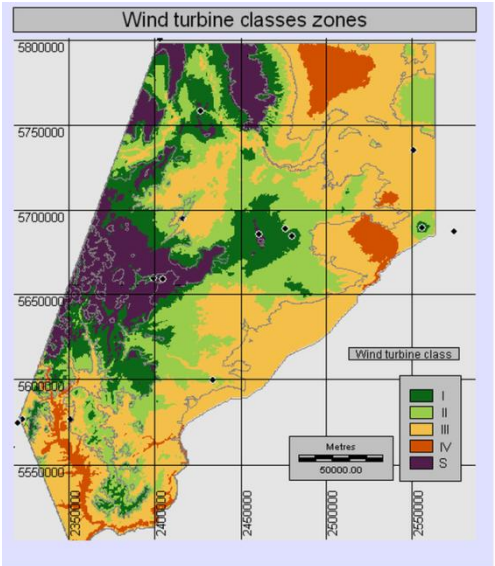

Figure 5: Zones suitable for the installation of Class I, II, III, IV and S wind turbines determined by the extreme wind regime at 120 m. The limit of the analysis area and topographic levels are also drawn.

3.3 CAPACITY FACTOR

Figure 6 shows three maps of the CF distribution for each class. Figure 6 (a) corresponds to the CF of the WT I-3300 type, which its average is 29.0 % ± 4.8 % and its maximum is 41.9 %. Figure 6 (b) shows the CF of the WT II-3300, its average value is 31.1 % ± 4.6 % and its maximum is 46.0 %. Finally, Figure 6 (c) corresponding to the CF of the WT III-3300 has an average value of 29.6 % ± 3.5 % and the maximum is 43.0 %.

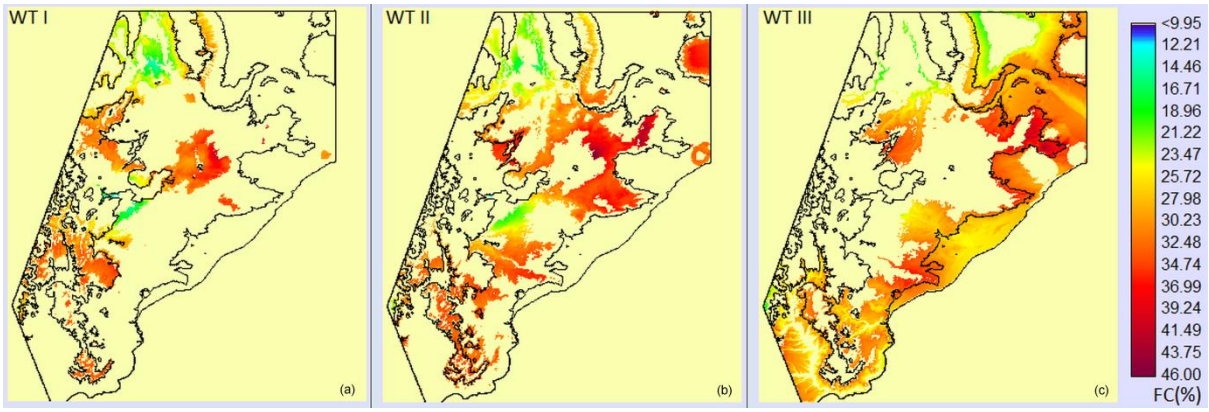

Figure 6: CF distribution (%) of the wind turbines. (a) WT I, (b) WT II and (c) WT III. The limit of the analysis area and topographic levels are also drawn.

In each class area, the surface whose CF exceeds 35 % is: 4.3 % (286 km^2) for WT I-3300; 16.1 % (1684 km^2) for WT II-3300; and 5.4 % (959 km^2) for WT III-3300. In Figure 7 it can be seen that WT II-3300 has the best performance of the four wind turbines because the curve shows a displacement to the greatest CFs.

Any wind turbine can operate in a lower class location, but never in a higher class. It was observed that if WT I-3300 is located in the zones of classes II or III its performance is lower than the other classes. This is because the sweep area of each wind turbine is the largest possible in its zone.

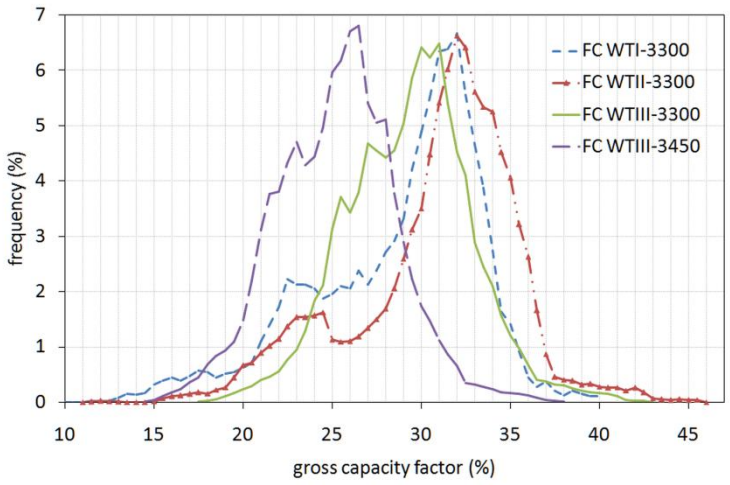

Figure 7: Distribution of CF in each wind turbine class.

In addition, Figure 7 shows that the turbine with the lowest performance is WT III-3450, with an average CF of 25.51 % ± 3.3 % and the maximum value is 38.3 %. These are lower than any of the other three turbines.

The CF of two wind turbines that are suitable for the same wind regime class but have different rated power were also compared and its results are shown in Figure 8. Even though WT III-3450 has a bigger rated power, the CF of WT III-3300 (Figure 8 (a)) turned out to be larger than WT III-3450. This is due to the difference in their power curves (Figure 9). For wind speeds that are lower than 10.0 m s-1 the curve of WT III-3300 is displaced to the left, taking advantage of weaker winds that are more frequent. On the other hand, WT III-3450 has a better performance between 10.5 and 12.0 m s^{-1} wind speed, however, these wind speeds are less frequent in its zone.

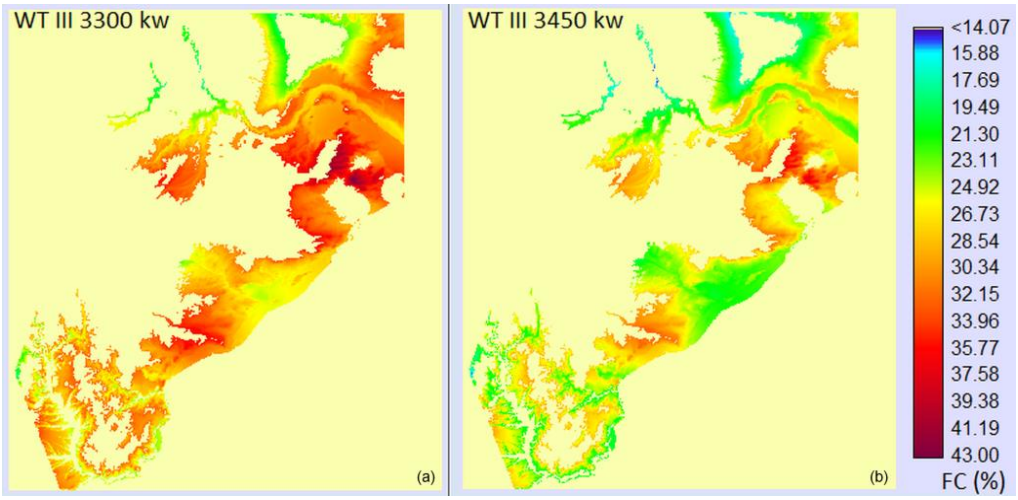

Figure 8: CF distribution (%) of the two Classes III wind turbines. (a) WT III-3300 kW and (b) WT III-3450 kW rated power.

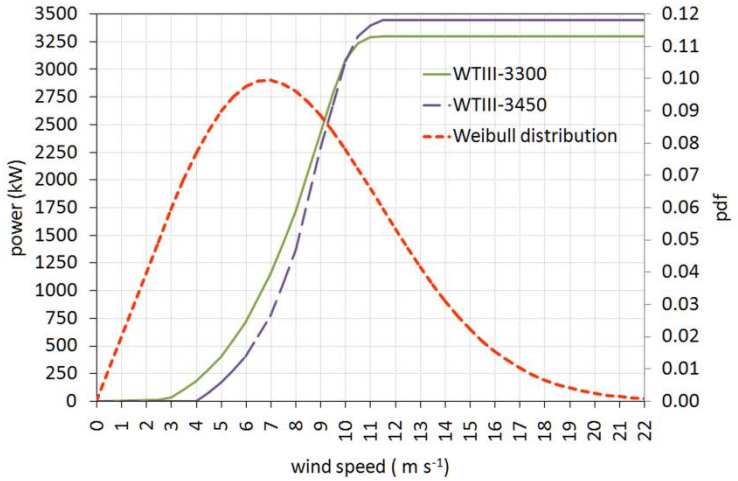

Figure 9: Power curves of wind turbines. Supplied by the manufacturer at a standard air density at sea level that is 1.225 kg m^{-3} (Source: https://www.thewindpower.net). The Weibull probability density function (pdf), at 120 m, which is characteristic of Class III wind regime, k = 2.17; c = 9.1 m s^{-1} and v = 8.1 m s^{-1}, is also shown.

IV. CONCLUSIONS

The wind resource map of Neuquén Province was updated in order to provide the basis for future studies to evaluate potential sites for the installation of wind farms. The previous wind map [1], at 50 m agl, was made with data from 12 meteorological stations and its spatial resolution was 1200 metres. In the update carried out, high quality wind data from 6 more sites (18 sites in total) were used and a high resolution (422 m) annual mean wind speed map was generated at 120 m agl. Also, the gross capacity factors of different classes and rated power of wind turbines were determined in order to compare their yields.

The studied region has a great variation of the wind regime. The near-surface wind speed varies between 3.95 m s^{-1} and 14.66 m s^{-1}, the highest values are located in the mountainous sector of the studied area. This occurs because of the strong dependence between the wind field and topography. The wind field obtained with the simulation has a satisfactory quality because r = 0.94 and εr < 8 %.

By making a Vref map at a height of 120 m agl, it was possible to determine the areas of use for the different classes of IEC wind turbines. The area with winds in which Class III wind turbines can be located has the largest extension.

WT II-3300 wind turbines had the best performance with the highest annual average CF (31.1 % ± 4.6 %), which is equivalent to a gross energy output of 9.0 GWh. WT I-3300 wind turbine has a CF = 29.0 % ± 4.8 % equivalent to a gross energy output of 8.4 GWh, WT III-3300 has a CF = 29.6 % ± 3.5 % equivalent to 8.6 GWh and WT III-3450 has a CF = 25.51 % ± 3.3 % equivalent to 7.7 GWh.

WT III-3450 has a lower performance than WT III-3300, which has a lower rated power, due to differences in power curves.

Class I wind turbines can be installed within an area of 6579 km^2, from which 286 km^2 have a CF > 35 % and 0.02 km^2 (696 ha) where the CF is greater than 40%. Class II has a total area of 10,435 km^2, with 1,684 km^2 where CF > 35 % and 0.31 km^2 (18,448 ha) where CF > 40 %. Class III (3300 kW) can be located in a total area of 17,716 km^2, from which 959 km^2 have a CF > 35 % and 0.09 km^2 (8757 ha) where the CF > 40 %. No zones have been detected where WT III-3450 has a CF > 38.5 %.

Results indicate that there are sites that have a very good to excellent wind resource to install wind farms.

ACKNOWLEDGEMENTS

The authors acknowledge the Invest Development Agency of Neuquén (ADI-NQN SEP) for providing the high-quality dataset used in the study. Also we acknowledge the Regional Wind Energy Centre that provided the ArgentinaMap software. The authors grateful to the Energy Entity of Neuquén Province (EPEN), National Weather Service of Argentina (SMN), Cutral Có Electric Cooperative, Capex Thermal Power Plant, Cutral Có Airport and Junín de los Andes Tech High School for the provision of wind data. This work was carried out with the fund of the Secretary of Science and Technology of the National University of Comahue (PI04/I227).

REFERENCES

[1]. Pedro G, Mattio HF, Palese C, Warchomicka N and Lassig JL (2006) Recurso eólico de la Provincia del Neuquén. Avances en Energías Renovables y Medio Ambiente, 10, 6.15 – 6.21.
[2]. Hualpa F and Milani F (2007) Mapa eólico de la Provincia de Mendoza. Report J-046, Mendoza: Universidad Tecnológica Nacional, Facultad Regional Mendoza, 60 pp.
[3]. Aires M, De Bortoli ME, Frigerio E, and Roko SR (2012) Estimación del potencial eólico de la provincia de Misiones. Avances en Energías Renovables y Medio Ambiente, 16, 06.09 – 06.16.
[4]. Guozden TM, Bianchi E, Solarte A and Mulleady C (2018) Evaluación de Recursos Eólicos en la Provincia de Río Negro (Patagonia Argentina) usando Merra Reanalysis. Meteorologica. 43, 2, 47 - 61.
[5]. Jurado A, Vinson E, Cerne B, Gill P and Nicchi F (2018) Factor de capacidad de turbinas eólicas en Argentina. Revista AEA de Ingeniería Electrica, 332: 54-58.
[6]. Barros V. R. (1983) Evaluación del potencial eólico de la Patagonia, Meteorologica, XIV, 1 and 2: 473-484.
[7]. Labraga J (1994) Extreme winds in the Pampa del Castillo Plateau, Patagonia, Argentina, with reference to wind farm settlement. Journal of Applied Meteorology, 33, 1: 85-95.
[8]. Lassig J L, Cogliat, MG, Bastanski MA and Palese C (1999) Wind characteristics in Neuquén, North Patagonia, Argentina. Journal of Wind Engineering and Industrial Aerodynamics, 79: 183-199.
[9]. Palese C, Lassig JL, Cogliati MG and Bastanski MA (2000) Wind regime and wind power in North Patagonia, Argentina. Wind Engineering, 24, 5: 361–377.
[10]. Brower M. (1998) WinMap was developed by Brower and Company, Andover, MA, USA.
[11]. Potts JR, Pierson SW, Maticen PP, Harnel JR and Babau VC (2001). Wind energy resource assessment of western and central Massachusetts. In Proceedings of American Institute of Aeronautics and Astronautics Congress, AIAA-2001-0060, 11pp.
[12]. Mattio HF and Tilca F (2009) Recomendaciones para mediciones de velocidad y dirección de viento con fines de generación eléctrica, y medición de potencia eléctrica generada por aerogeneradores. Report for CREE, INENCO, Ministerio de Planificación Federal Inversión Pública y Servicios, Secretaría de Energía de la Nación. 33 pp.
[13]. Wilks D S (1995) Statistical methods in the atmospheric sciences. An introduction. Academic Press, 467 pp.
[14]. IEC International Electrotechnical Commission (2005) 61400-1; Wind turbines – Part 1: Design requirements. 92 pp.